Glutathione content and expression of proteins involved with glutathione metabolism differs in longissimus dorsi, subcutaneous adipose, and liver tissues of finished vs. growing beef steers[1]

Jing Huang,[†] Yang Jia,[†] Qing Li,[†] Kwangwon Son,[†] Charles Hamilton,[†] Walter R. Burris,[†] Phillip J. Bridges,[†] Arnold J. Stromberg,[‡] and James C. Matthews[†,2]

[†]Department of Animal and Food Sciences, University of Kentucky, Lexington, KY 40546; and [‡]Department of Statistics, University of Kentucky, Lexington, KY 40536

ABSTRACT: Increased tissue redox state may result in sub-optimal growth. Our goal was to determine if glutathione (**GSH**) content and expression of proteins involved with GSH metabolism change in longissimus dorsi (**LD**), subcutaneous adipose (**SA**), and liver tissues of growing vs. finishing steer phenotypes. Tissues were taken from 16 Angus steers (BW = 209 ± 29.4 kg) randomly assigned (n = 8) to develop through Growing (final BW = 301 ± 7.06 kg) vs. Finished (final BW = 576 ± 36.9 kg) growth phases, and at slaughter had achieved different rib-eye area (REA) (53.2, 76.8 cm^2), marbling scores (296, 668), and 12th rib adipose thickness (0.54, 1.73 cm), respectively (Amino Acids, doi:10.1007/s00726-018-2540-8). GSH content (mg/g wet tissue) was determined by a commercial assay and the relative content of target protein and mRNA in tissue homogenates was determined by Western blot and reverse-transcribed PCR analyses, respectively. The effect of growth phase (Finished vs. Growing) was assessed by ANOVA using the GLM procedure of SAS. The LD of Finished steers had more ($P < 0.04$) GSH (42%) and GSH synthesizing (GCLC, 61%; GCLM, 21%) and metabolizing (GPX1, 42%; GPX3, 73%; GGT1, 56%) enzymes, and less ($P < 0.02$) GPX2 (46%), EAAC1 (30%) and glutamine synthetase (GS) (28%), whereas GTRAP3-18 and ARL6IP1 did not differ ($P > 0.57$). Principal component analysis found that GSH content of LD was associated with REA and marbling score. The SA of Finished steers had less ($P < 0.04$) GSH (38%), GSH metabolizing (GPX4, 52%; GGT1, 71%) enzyme mRNA, and GTRAP3-18 (123%) and ARL6IP1 (43%), whereas the mRNA content of GSH-synthesizing enzymes and content of EAAC1 and GS did not differ ($P > 0.32$). The liver of Finished steers had less ($P < 0.02$) mRNA content of GSH synthesizing (GCLC, 39%; GSS 29%) and metabolizing (GPX1, 30%) enzymes, and more ($P < 0.01$) GSTM1 metabolizing enzyme (114%). The change in GSH content as steers fattened indicate an increased antioxidant capacity in the LD of Finished steers, and a decreased antioxidant capacity in SA, consistent with changes in enzyme and transporter expression. Changes in liver enzyme and transporter expression were consistent with no change in GSH content. The relationship of EAAC1 regulatory proteins (GTRAP3-18, ARL6IP1) to GSH, EAAC1, and GS content differs and changes as Growing steers develop into Finished phenotypes. These findings provide mechanistic insight into how antioxidant capacity occurs in tissues of economic and metabolic importance as cattle fatten.

Key words: adipose, cattle, EAAC1, glutathione, liver, muscle

[1]This is publication no. 18-07-069 of the Kentucky Agricultural Experiment Station and is published with approval of the director. This work is supported by the National Institute of Food and Agriculture, U.S. Department of Agriculture, AFRI project no. 11303353 (J.C.M., R.W.B.), The Kentucky Cattlemen's Association (J.C.M., R.W.B., P.J.B.), and the National Institutes of Health, General Medical Sciences project no. P20GM103436 (A.J.S.).

[2]Corresponding author: jmatthew@uky.edu

Received April 28, 2018.
Accepted September 6, 2018.

J. Anim. Sci. 2018.96:5152–5165
doi: 10.1093/jas/sky362

INTRODUCTION

The tissues of fattened vs. lean animals likely experience more oxidative stress, which may result in sub-optimal growth (Noeman et al., 2011; Moisa et al., 2013; Jankovic et al., 2014). Glutathione (γ-L-glutamyl-L-cysteinylglycine, **GSH**) functions as a major antioxidant to protect organisms against oxidative damage (Schmidt and Dringen, 2012). In obese vs. normal mice and humans, the GSH content of skeletal muscle and adipose tissues is decreased (Anderson et al., 2009; Jankovic et al., 2014). Changes in tissue GSH concentrations reflect altered oxidative stress levels and result from net changes in GSH production and use (e.g., glutathione peroxidases [GPX] 1 to 4 events (Lu, 2013)). GSH synthesis depends on expression of rate-limiting γ-glutamate-cysteine ligase and the availability of Glu and Cys (Sato et al., 1999; Flaring et al., 2003), which are substrates of two (EAAC1 and GLT-1) system X^-_{AG} activity transporters.

Knowledge of how shifts in biochemical capacities occur to support putative changes in antioxidant capacity accompanying altered compositional gain in economically important tissues of cattle as they fatten may identify target proteins for manipulation. In neurons, the interaction between GTRAP3-18 and ARL6IP1 affects EAAC1 activity and cellular GSH levels (Watabe et al., 2008; Aoyama and Nakaki 2012). In the liver of finished vs. growing beef steers, system X^-_{AG} activity, EAAC1 content, and glutamine synthetase (**GS**) activity and content are decreased; GTRAP3-18 and ARL6IP1 contents are increased; whereas GSH and GLT-1 contents do not differ (Huang et al., 2018). The goals of this study were to (1) test the hypothesis that the content of GSH in longissimus dorsi (**LD**) and subcutaneous adipose (**SA**) tissues would be less in these finished vs. growing steers and (2) gain insight into the mechanisms by which tissue GSH content was achieved by elucidating related mechanisms.

MATERIALS AND METHODS

All procedures involving animals were approved by the University of Kentucky Institutional Animal Care and Use Committee.

Animal Model, Slaughter, Tissue Collection, and Carcass Evaluation

The animal management regimen and model for steers that yielded the tissues for the present experiment have been reported (Huang et al., 2018). Briefly, 16 weaned, predominately Angus, steers of similar shrunk (denied feed and water for 14 h) BW (209 ± 29.4 kg) were randomly assigned (n = 8) to either Growing (target BW = 295 kg) or Finished (target BW = 568 kg) treatment groups. Steers were individually fed (Calan gates in a dry-lot barn) enough of a diet that contained (% as-fed) cracked corn (60), cottonseed hulls (20), soybean meal (7), soybean hulls (5), dried distiller's grain (2), alfalfa meal (2), glycerin (2), limestone (1.5), and urea (0.5) to support 1.51 kg gain/d (NRC, 1996) throughout the trial. Steers had ad libitum access to fresh water and a vitamin–mineral mix (UK IRM Beef Cattle Vitamin-mineral Mix, Burkmann Mill, Inc., Danville, KY). As previously described in detail (Huang et al., 2018), Growing steers required 57 ± 7 d to reach their final BW (301 ± 7.06 kg) and 261 ± 12 d were required for Finished steers to reach their final BW (576 ± 36.9 kg). As planned, the ADG did not differ (1.51 vs. 1.46 kg/d) in Growing vs. Finished steers.

The methods used for the slaughter, tissue collection, and carcass evaluation of Growing and Finished steers have been reported (Huang et al., 2018). Briefly, one steer per day was slaughtered, from alternating treatment groups. Steers were stunned by captive bolt pistol and then exsanguinated to allow recovery of carcasses for consumption. After the HCW was recorded, liver, LD (between 12th and 13th rib) muscle and its adjacent SA tissue were collected as described (Brown et al., 2009). For determination of GSH content (Huang et al., 2018), fresh tissues were homogenized in 5% ice-cold metaphosphoric acid solution followed by centrifugation at 3,000 × g, 4°C for 10 min. The supernatant was collected and stored at −80°C overnight for next day assay (see below). For all other analyses, tissue samples were placed in foil packs, snap-frozen in liquid nitrogen, and stored at −80°C until assayed for RNA and protein expression.

Twenty-four hours postmortem, carcass evaluations were conducted on the right side of the carcass according to USDA standards (USDA, 1997).

As described previously in detail (Huang et al., 2018), Finished steers had greater BW (91%), HCW (107%), ribeye area (44%), 12th rib adipose (220%), marbling score (126%), yield grade (71%), and whole-liver wet weight (44%), while the percentage of KPH adipose tissue tended to be greater. In contrast, whole-liver wet weight/100 kg of final BW was 25% less in Finished vs. Growing steers.

Western Blot Analysis

In general, Western blot analysis of relative amount of targeted proteins was conducted as described by this research group (Howell et al., 2001; Miles et al., 2015). For liver homogenates, 1 g of tissue was homogenized on ice for 30 s (setting 11, POLYTRON, Model PT10/35; Kinematic, Inc., Neuchâtel) in 7.5 mL of 4°C sample extraction buffer solution (0.25 m*M* sucrose, 10 m*M* HEPES–KOH pH 7.5, 1 m*M* EDTA, and 50 µL of protease inhibitor (Sigma, St. Louis, MO). Protein was quantified by a modified Lowry assay, using bovine serum albumin as a standard (Kilberg, 1989). Proteins were separated by 12% SDS–PAGE, followed by electrotransfer to a 0.45-µm nitrocellulose membrane (Bio-Rad, Hercules, CA). Blots were stained with Fast-Green (Fisher, Pittsburgh, PA) and the relative amount of stained protein per lane/sample determined by densitometric analyses and recorded as arbitrary units (Howell et al., 2001; Miles et al., 2015).

The relative protein content of EAAC1, GLT-1, GTRAP3-18, ARL6IP1, and GS in tissue homogenates was evaluated by immunoblot analyses as described (Brown et al., 2009; Miles et al., 2015, Huang et al., 2018). Briefly, blots were hybridized with 1 µg of IgG antihuman EAAC1 polyclonal anti-body (Santa Cruz Biotechnology, Inc., Santa Cruz, CA), 1 µg of IgG anti-rabbit GLT-1 polyclonal antibody (Abcam Inc., Cambridge, MA), 4 µg of IgG antihuman GTRAP3-18 (Abcam Inc., Cambridge, MA), and 5 µg of IgG antihuman ARL6IP1 (Abgent Inc., San Diego, CA), respectively, per milliliter of blocking solution (1% nonfat dry milk [wt/vol] in 30 mM Tris-Cl, 200 mM NaCl, 0.1% Tween 20 [vol/vol], pH 7.5) for 1.5 h at room temperature with gentle rocking. For GS detection, blots were hybridized with 1.25 µg of IgG anti-sheep polyclonal antibody (BD Biosciences, San Jose, CA) per milliliter of blocking solution (5% nonfat dry milk [wt/vol], 10 mM Tris-Cl [pH 7.5], 100 mM NaCl, 0.1% Tween 20 [vol/vol]) for 1 h at 37°C with gentle rocking.

All protein–primary antibody binding reactions were visualized with a chemiluminescence kit (Pierce, Rockford, IL) after hybridization of primary antibodies with horseradish peroxidase–conjugated donkey antirabbit IgG (Amersham, Arlington Heights, IL; GLT-1, EAAC1 and ARL6IP1, 1:5,000); horseradish peroxidase-conjugated goat antimouse IgG (BD Biosciences, San Jose, CA; glutamine synthetase, 1:5,000); and horseradish peroxidase–conjugated donkey antigoat IgG (Santa Cruz Biotechnology; GTRAP3–18, 1:5,000).

Densitometric analysis of immunoreactive products was performed as described previously (Howell et al., 2003; Fan et al., 2004; Xue et al., 2011). Briefly, after exposure to autoradiographic film (Amersham, Arlington Heights, IL), a digital image of the radiographic bands was recorded and quantified as described (Swanson et al., 2000). Apparent migration weights (M_r) were calculated by regression of the distance migrated against the M_r of a 16- to 185-kDa standard (Gibco BRL, Grand Island, NY) using the Versadoc imaging system (Bio-Rad) and Quantity One software (Bio-Rad). Band intensities of all observed immunoreactive species (one for GTRAP3-18, ARL6IP1, and GS; two for EAAC1, whereas GLT-1 immunoreactive species were not detected) within a sample were quantified by densitometry (as described above for Fast-Green stained proteins) and reported as arbitrary units. Densitometric data were corrected for unequal (≤14%) loading, transfer, or both, and amount of detected protein normalized to relative amounts of Fast-Green-stained proteins common to all immunoblot lanes/samples (Miles et al., 2015). Digital images were prepared using PowerPoint software (Microsoft, PowerPoint 2003, Bellvue, MA).

GSH Content in LD and SA Tissues

As described before for liver tissue (Huang et al., 2018), upon collection, LD and subcutaneous fat tissues (0.30 to 0.35 g) were rinsed in 0.9% (wt/vol) NaCl solution and homogenized in 2.5 mL 5% (wt/vol) ice-cold metaphosphoric acid solution. The homogenates were then centrifuged at 3,000 × g, 4°C for 10 min. After centrifugation, 100 to 200 µL of supernatant was collected and stored at −80°C overnight for use the next day.

The content of reduced GSH in tissues was determined using the GSH-400 kit (Oxis International Inc., Beverly Hills, CA), following the manufacturer's instructions. For LD, a standard curve of 0, 20, 40, 60, and 80 µmol/L GSH was

used. For SA, a standard curve of 0, 4, 8, 12, 16, and 20 μmol/L GSH was used. The final absorbance at 400 nm was measured using a Genesys 20 spectrometer (Thermo Electron Corp., Waltham, MA). Samples were assayed in triplicate and values are reported as mg GSH/g wet tissue.

RNA Extraction and Analysis

Total RNA was extracted from frozen LD, SA, and liver tissues using TRIzol Reagent (Invitrogen Corporation, Carlsbad, CA) following the manufacturer's instructions. The purity and concentration of total RNA samples was analyzed by a NanoDrop ND-1000 Spectrophotometer (NanoDrop Technologies, Wilmington, DE), which revealed that all samples were of high purity with 260:280 nm absorbance ratios of 2.0 to 2.1 and 260:230 nm absorbance ratios ranging from 1.5 to 1.9. The integrity of total RNA was examined by gel electrophoresis using an Agilent 2100 Bioanalyzer System (Agilent Technologies, Santa Clara, CA) at the University of Kentucky Microarray Core Facility (Lexington, KY). Visualization of gel images and electropherograms showed that all RNA samples were of high quality with 28S:18S rRNA ratios greater than 1.8 and RNA integrity numbers greater than 8.5.

Real-Time Reverse-Transcribed (RT) PCR Analysis

Real-time RT-PCR was performed to determine the relative expression of mRNA using an Eppendorf Mastercycler ep realplex2 system (Eppendorf, Hamburg, Germany) with iQ SYBR Green Supermix (Bio-Rad). Briefly, cDNA was synthesized using the SuperScript III 1st Strand Synthesis System (Invitrogen), with 0.5 μg of RNA used for each reverse transcription reaction. Real-time RT-PCR was performed with a total volume of 25 μL per reaction, with each reaction containing 5 μL of cDNA, 1 μL of a 10-μM stock of each primer (forward and reverse), 12.5 μL of 2× SYBR Green PCR Master Mix, and 5.5 μL of nuclease-free water. The resulting real-time PCR products were purified using a PureLink Quick Gel Extraction Kit (Invitrogen) and sequenced at Eurofins Scientific (Eurofins, Louisville, KY). Sequences were compared with the corresponding RefSeq mRNA sequences that were used as templates for primer set design. The sequences of the primers (Supplementary Table 1) and the resulting sequence-validated real-time PCR reaction amplicons (Supplementary Fig. 1) are presented in the Supplementary data file. The relative mRNA content was normalized to the geometric means of three constitutively expressed genes whose CT values were not affected ($P > 0.43$) by growth phase. Beta-actin (ACTB), glyceraldehyde 3-phosphate dehydrogenase (GAPDH), and ubiquitin C (UBC) were used as the calibrating genes in LD; ACTB, GAPDH, and peptidylprolyl isomerase A (PPIA) were used as the calibrating genes in SA tissue; and TATA-box-binding protein (TBP), GAPDH, and tyrosine 3-monooxygenase (YWHAZ) were used as calibrating genes in liver tissue. RT-PCR reactions were run in triplicate and gene expression was analyzed by the 2ΔΔCT method (Livak and Schmittgen, 2001).

Statistical Analysis

Individual steers were the observational units. Data were analyzed as a completely randomized design by ANOVA using the GLM procedures of SAS (SAS Inst. Inc., Cary, NC). All data were analyzed in a one-way ANOVA model to test for Finished vs. Growing treatment effects. Treatment differences were considered significant at the $\alpha = 0.05$ level. Eight observations were made for each tissue and all parameters, except that only four observations per treatment were made for RT-PCR analysis of SA tissue gene expressions (Table 4) due to freezer failure. Principal component analysis (**PCA**) was performed using JMP Pro software (version 14; SAS Inst. Inc.). As appropriate, ADG, carcass traits, relative mRNA abundance, and relative protein abundance in liver, LD, and SA tissues were used as input variables for PCA.

RESULTS

Longissimus Dorsi

The GSH content (mg/g wet tissue) in LD tissue was greater (42%, $P < 0.01$) in Finished vs. Growing steers (Table 1). Densitometry analysis of Western blot (Fig. 1) data of LD homogenates (Table 1) showed less EAAC1 (30%, $P = 0.02$) and GS (28%, $P = 0.02$) content in Finished vs. Growing steers, whereas GTRAP3-18 ($P = 0.80$) and ARL6IP1 ($P = 0.57$) did not differ. The presence of GLT-1 was not detected in LD (data not shown).

The relative abundance of mRNA for GSH-synthesizing proteins in LD was greater for GCLC (61%, $P = 0.004$) and GCLM (29%, $P = 0.001$) in

Table 1. Comparison of GSH, EAAC1, GTRAP3-18, ARL6IP1, and GS content in LD tissues of Growing vs. Finished Angus steers

	Growing	Finished	SEM[3]	*P*-value
Metabolites				
GSH[1]	0.24	0.34	0.02	<0.01
Protein[2]				
EAAC1	10,689	7,443	972	0.02
GTRAP3-18	2,969	3,102	363	0.80
ARL6IP1	6,755	5,821	1,285	0.57
GS	8,298	5,935	700	0.02

[1]Values are mg/g wet tissue.

[2]Values (arbitrary densitometric units) are means (n = 8) and pooled SEM of relative GSH, EAAC1, GTRAP3-18, ARL6IP1, and GS content in LD homogenates (Fig. 1) of growing (BW = 301 kg) and finished (BW = 576 kg) Angus steers. Values were determined by densitometric quantification of immunoreactive species identified by Western blot analyses (Fig. 1).

[3]Most conservative error of the mean.

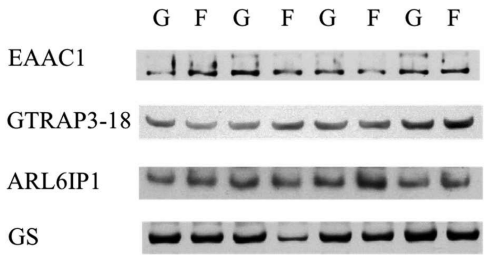

Figure 1. Western blot analysis of EAAC1, GTRAP3-18, ARLI6P1, and GS in LD homogenates (15 µg per lane) of Growing (G) and Finished (F) steers. Data are representative of eight Growing and eight Finished steers (as described in Table 1). The apparent migration weights (kDa) for proteins were 70 for the lower, and 89 for the higher, predominant immunoreactants for EAAC1; 42 for GTRAP3-18; 21 for ARL6IP1; and 43 for GS; respectively.

Finished vs. Growing steers, but did not differ for GSS (P = 0.146) and GSR (P = 0.837) (Table 2). For GSH-metabolizing proteins, GPX1 (61%, P = 0.004), GPX3 (29%, P = 0.001) and GGT1 (56%, P = 0.045) mRNA abundance was greater in Finished vs. Growing steers, whereas GPX2 (46%, P < 0.001) expression was less and GPX4 expression tended to be less (P = 0.090).

Subcutaneous Adipose

The content of GSH in SA tissue (Table 3) was decreased (38%, P = 0.04) in Finished vs. Growing steers. Concomitantly, densitometric analysis of Western blot data (Fig. 2) of SA tissue homogenates (Table 3) found increased GTRAP3-18 (123%, P = 0.03) and ARL6IP1 (43%, P = 0.01) content in Finished vs. Growing steers, whereas EAAC1 (P = 0.11) and GS content (P = 0.37) did not differ. The presence of GLT-1 was not detected in SA (data not shown).

For GSH-synthesizing proteins, the relative abundance of GCLC, GCLM, GSS, and GSR mRNA did not differ (P ≥ 0.261) in the SA tissue of Finished vs. Growing steers (Table 4). For GSH-metabolizing proteins, the relative content was less for GPX4 (52%, P = 0.013) and GGT1 (71%, P = 0.001) mRNA, whereas GPX1 (P = 0.319) and GPX3 mRNA abundance did not differ (P = 0.101), in Finished vs. Growing steers.

Liver

The GSH content in liver tissue did not differ (P = 0.96) between Finished and Growing steers (Table 5; Huang et al., 2018). For GSH-synthesizing proteins in liver (Table 5), real-time RT-PCR analysis found less GCLC (39%, P = 0.024) and GSS (29%, P = 0.009) mRNA content in Finished vs. Growing steers, whereas GCLM (P = 0.683) and GSR mRNA (P = 0.354) did not differ.

For GSH-metabolizing proteins in liver, real-time RT-PCR assays showed less GPX1 (30%, P = 0.001) but more GSTM1 (113%, P = 0.001) mRNA, whereas GGT1 mRNA tended to be greater (P = 0.077) and mGST3 mRNA did not differ (P = 0.254) in Finished vs. Growing steers. For GSH exporter proteins in liver tissue, mRNA abundance was less for ABCC1 (39%, P = 0.001), SLCO2B1 (61%, P = 0.025), and SLCO1B3 (32%, P = 0.001) in Finished vs. Growing steers.

Principal Component Analysis

PCA of the potential correlation between carcass traits and other analytes (Fig. 3) indicated that PC 1 and PC 2 explained 49.3% of the variation. All steers sorted into their respective development stage in PC 1 (36.3% of total variation). In contrast, two steers from each development stage segregated within the positive quadrants of PC 2, whereas six steers from each development stage segregated into the negative quadrants of PC 2.

Table 2. Real-time RT-PCR analysis of the relative content of GSH-synthesizing and metabolizing protein mRNA by LD from Growing vs. Finished Angus steers[1]

Protein[2]	Growing	Finished	SEM[3]	*P*-value[4]
GSH-synthesizing protein				
GCLC	0.94	1.51	0.12	<0.01
GCLM	0.96	1.24	0.05	<0.01
GSS	1.01	0.90	0.06	0.15
GSR	1.05	1.09	0.18	0.84
GSH-metabolizing protein				
GPX1	1.04	1.48	0.12	0.02
GPX2	1.01	0.55	0.06	<0.01
GPX3	1.05	1.81	0.12	<0.01
GPX4	1.02	0.83	0.08	0.09
GGT1	1.06	1.65	0.24	0.04

[1]Values are mRNA content in LD of Growing (n = 8, BW = 301 kg) and Finished (n = 8, BW = 576 kg) steers normalized to the geometric mean of three constitutively expressed reference genes: β-actin (ACTB), glyceraldehyde 3-phosphate dehydrogenase (GAPDH), and ubiquitin C (UBC).

[2]Gene symbols: GCLC (γ-glutamate-cysteine ligase catalytic subunit); GCLM (γ-glutamate-cysteine ligase modifier subunit); GSS (glutathione synthetase); GSR (GSSG reductase); GPX1 (glutathione peroxidase 1); GPX2 (glutathione peroxidase 2); GPX3 (glutathione peroxidase 3); GPX4 (glutathione peroxidase 4); GGT1 (γ-glutamyltranspeptidase 1).

[3]Most conservative error of the mean.

[4]*P*-values were obtained from ANOVA *F*-test.

Table 3. Comparison of GSH, EAAC1, GTRAP3-18, ARL6IP1, and GS content in SA tissue of Growing vs. Finished Angus steers

	Growing	Finished	SEM[3]	*P*-value
Metabolite				
GSH[1]	0.13	0.08	0.02	0.04
Protein[2]				
EAAC1	8,774	6,117	1,317	0.11
GTRAP3-18	4,069	9,084	1,667	0.03
ARL6IP1	19,264	27,471	2,348	0.01
GS	7,004	5,826	953	0.37

[1]Values are mg/g wet tissue.

[2]Values (arbitrary densitometric units) are means (n = 8) and pooled SEM of relative GSH, EAAC1, GTRAP3-18, ARL6IP1, and GS content in SA tissue homogenates (Fig. 2) of Growing (BW = 301 kg) and Finished (BW = 576 kg) Angus steers. Values were determined by densitometric quantification of immunoreactive species identified by Western blot analyses (Fig. 2).

[3]Most conservative error of the mean.

Principal component analysis of only GSH tissue content and carcass traits (REA, YG, SA [12th rib], marbling score; Fig. 4) indicated that PC 1 and PC 2 explained 73.9% of the variation and that the LD GSH content, REA, marbling score, SA, YG, and HCW were strongly ($r \geq 0.80$) correlated with PC 1 and not ($r \leq 0.13$) correlated with PC 2. In contrast, liver GSH content was not ($r = 0.06$) correlated with PC 1, and moderately ($r = 0.75$) correlated with PC 2, whereas SA GSH content was moderately and negatively correlated with PC 1 ($r = -0.63$) and PC 2 ($r = -0.64$).

Principal component analysis of the potential correlation between only LD-specific carcass traits (REA, marbling score), GSH, and mRNA contents (Fig. 5) indicated that PC 1 and PC 2 explained 57.6% of the variation and revealed a moderate to strong ($0.52 \leq r \leq 0.93$) correlation between PC 1 and REA, marbling score, the relative content of mRNA for genes responsible for regulation of GSH synthesis (γ-glutamate-cysteine ligase modifying subunit, GCLM) and X_{AG}^{-} activity (GTRAP3-18, ARL6IP1), and use of GSH (GPX1, GPX3). In contrast, these variables were not ($r < 0.20$) or weakly ($0.22 \leq r \leq 0.40$) correlated with PC 2.

The content of GSH and the catalytic unit of γ-glutamate-cysteine ligase (GCLC) mRNA in LD were strongly ($r = 0.80$) correlated with PC 1 and not ($r = -0.18$) correlated with PC 2. In contrast, the mRNA content of GSH synthetase was weakly and negatively correlated with PC 1 ($r = -0.39$) and PC 2 ($r = -0.36$), whereas GSH reductase was not ($r = 0.15$) correlated with PC 1 and strongly ($r = 0.89$) correlated with PC 2. In terms of GSH

users, mRNA content of GPX2 was strongly (r = −0.80) correlated with PC 1 and weakly (r = 0.39) correlated with PC 2, whereas GPX4 was weakly (r = −0.44) correlated with PC 1, moderately (r = 0.71) correlated with PC 2.

DISCUSSION

GSH Metabolism

Our understanding of how cells maintain the capacity to respond to shifts in antioxidant challenges associated with shifting metabolic demands of healthy animals is incomplete and remains a fundamental question of growth biology. However, it is known that there is a difference between chronic (typically deleterious) and low-amplitude transient (involved in metabolic pathway signaling) oxidative stress challenges (Galinier et al., 2006) and that oxidative stress promotes changes in metabolic balance and efficiency of nutrient use (Elsasser et al., 2008). Moreover, a fundamental hypotheses associated with animal fattening is that an increased redox state (generation of more reactive oxygen species than can be reduced by enzymatic and non-enzymatic antioxidant systems) may result in sub-optimal growth (Vincent et al., 2007; Noeman et al., 2011; Moisá et al., 2013; Furukawa et al., 2017).

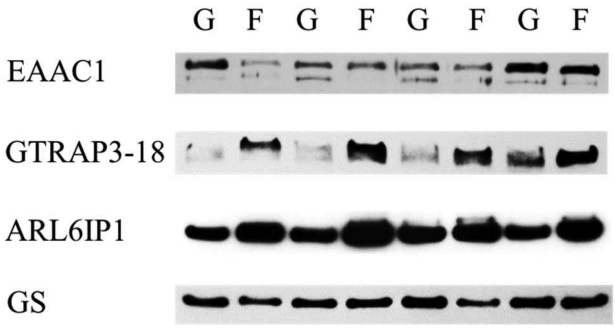

Figure 2. Western blot analysis of EAAC1, GTRAP3-18, ARLI6P1, and GS in SA tissue homogenates (15 µg per lane) of Growing (G) and Finished (F) steers. Data are representative of eight Growing and eight Finished steers (as described in Table 2). The apparent migration weights (kDa) for proteins were 70 for the lower, and 89 for the higher, predominant immunoreactants for EAAC1; 42 for GTRAP3-18; 21 for ARL6IP1; and 43 for GS; respectively.

GSH is the most abundant cellular thiol present in mammalian tissues and serves as a major antioxidant in animal tissues (Aoyama et al., 2008; Forman et al., 2009; Schmidt and Dringen, 2012). The capacity for thiol-based redox systems is determined by the interplay between enzyme system-based producers of H_2O_2 (e.g., NADH and NADPH oxidases; mitochondrial complexes I, I, and III; and superoxide dismutases) and GSH-mediated users of H_2O_2 (GSH peroxidase 1 to 8, thioredoxin 1 to 3) (Sies et al., 2017).

The content of GSH in a given tissue is the net balance resulting from GSH synthesis minus GSH use. GSH synthesis involves two consecutive enzymatic reactions: formation of γ-glutamylcysteine from Glu and Cys by γ-glutamylcysteine ligase (the rate-limiting reaction) and formation of GSH from γ-glutamylcysteine and glycine by GSH synthase. γ-Glutamylcysteine ligase is composed of a catalytic subunit (GCLC) and a modifier subunit (GCLM) (Yang et al., 2002; Franklin et al., 2009). The

Table 4. Real-time RT-PCR analysis of the relative content of GSH-synthesizing and metabolizing protein mRNA by SA tissues from Growing vs. Finished Angus steers[1]

Protein[2]	Growing	Finished	SEM[3]	*P*-value[4]
GSH-synthesizing protein				
GCLC	1.10	0.90	0.27	0.60
GCLM	1.01	1.01	0.12	0.99
GSS	1.04	0.72	0.16	0.26
GSR	1.02	1.21	0.14	0.32
GSH-metabolizing protein				
GPX1	1.00	1.17	0.16	0.32
GPX3	1.04	1.92	0.42	0.10
GPX4	1.02	0.49	0.11	0.01
GGT1	1.02	0.30	0.11	< 0.01

[1]Values are mRNA content in SA tissues of Growing (n = 4, BW = 301 kg) and Finished (n = 4, BW = 576 kg) steers normalized to the geometric mean of three constitutively expressed genes: β-actin (ACTB), glyceraldehyde 3-phosphate dehydrogenase (GAPDH), and peptidylprolyl isomerase A (PPIA).

[2]Gene symbols: GCLC (γ-glutamate-cysteine ligase catalytic subunit); GCLM (γ-glutamate-cysteine ligase modifier subunit); GSS (glutathione synthetase); GSR (GSSG reductase); GPX1 (glutathione peroxidase 1); GPX3 (glutathione peroxidase 3); GPX4 (glutathione peroxidase 4); GGT1 (γ-glutamyltranspeptidase 1).

[3]Most conservative error of the mean.

[4]*P*-values were obtained from ANOVA *F*-test.

Table 5. Relative content of GSH-synthesizing and metabolizing protein mRNA in liver tissue of Growing vs. Finished Angus steers[1]

Protein[2]	Growing	Finished	SEM[3]	*P*-value[4]
Metabolite				
GSH[5]	1.08	1.07	0.09	0.96
GSH-synthesizing protein				
GCLC	1.07	0.65	0.14	0.02
GCLM	0.95	0.91	0.07	0.68
GSS	1.03	0.73	0.09	0.01
GSR	1.02	0.92	0.08	0.35
GSH-metabolizing protein				
GPX1	1.01	0.71	0.06	<0.01
GSTM1	0.93	1.99	0.20	<0.01
mGST3	1.02	1.12	0.07	0.25
GGT1	1.04	1.27	0.10	0.08
GSH/GSSG exporter protein				
ABCC1	1.02	0.62	0.07	<0.01
SLCO1B3	0.95	0.65	0.05	<0.01
SLCO2B1	1.24	0.48	0.26	0.02

[1]Values are mRNA content in liver tissue of Growing (n = 8, BW = 301 kg) and Finished (n = 8, BW = 576 kg) steers normalized to the geometric mean of three constitutively expressed genes: TATA-box binding protein (TBP), glyceraldehyde 3-phosphate dehydrogenase (GAPDH), and tyrosine 3-monooxygenase (YWHAZ).

[2]Gene symbols: GCLC (γ-glutamate-cysteine ligase catalytic subunit); GCLM (γ-glutamate-cysteine ligase modifier subunit); GSS (glutathione synthetase); GSR (GSSG reductase); GPX1 (glutathione peroxidase 1); GSTM1 (glutathione-S-transferase M1 subunit); mGST3 (microsomal glutathione-S-transferase 3); GGT1 (γ-glutamyltranspeptidase 1); ABCC1 (ATP-binding cassette, sub-family C (CFTR/MRP), member 1); SLCO1B3 (solute carrier organic anion transporter family, member 1B3); and SLCO2B1 (solute carrier organic anion transporter family, member 2B1).

[3]Most conservative error of the mean.

[4]*P*-values were obtained from ANOVA *F*-test.

[5]Values are mg/g wet tissue and are from Huang et al. (2018).

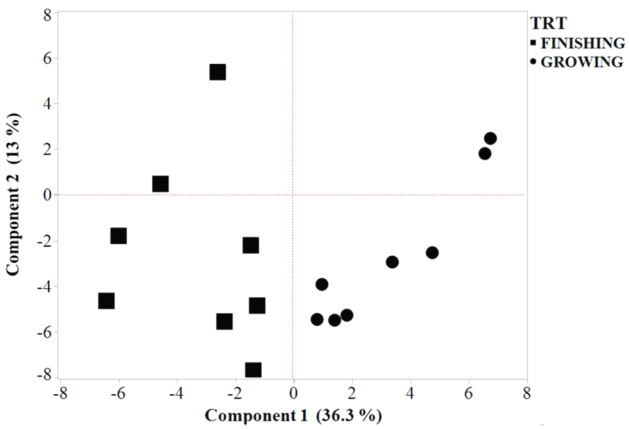

Figure 3. Score plot from principal component analysis showing the correlation of the first two principal components (Components 1 and 2) among development stage (Growing vs. Finished) of steers and carcass traits, GSH content, and relative mRNA and protein abundance in liver, LD, and SA tissues.

γ-glutamylcysteine ligase catalyzer subunit catalyzes γ-glutamylcysteine synthesis, whereas GCLM modulates GCLC activity by lowering the K_m for Glu and increasing the K_i for the feedback inhibition of γ-glutamylcysteine by GSH (Richman and Meister, 1975; Huang et al., 1993a,b; Chen et al., 2005).

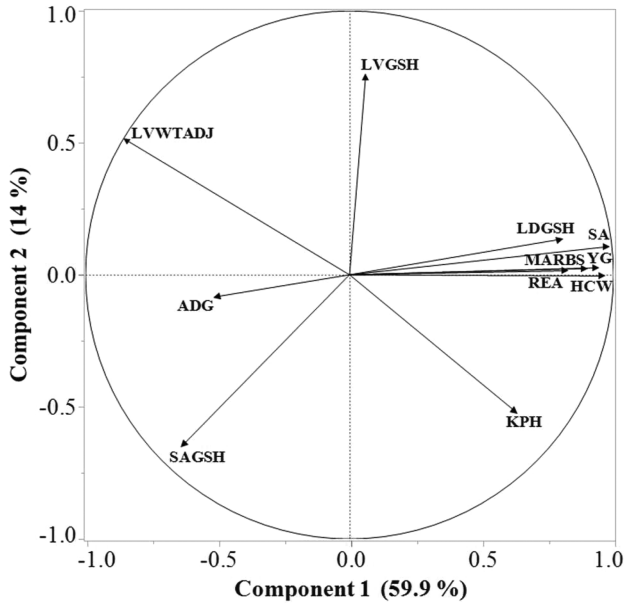

Figure 4. Loading plot from principal component analysis of steer (Growing and Finished steers) parameters showing the correlation of the first two principal components (Components 1 and 2) among tissue GSH contents and growth performance and carcass traits. LVGSH, liver GSH content; LVWTADJ, liver weight, g/100 kg BW); LDGSH, LD GSH content; MARBS, marbling score; SA, 12th to 13th rib SA thickness (cm); SAGSH, 12th rib SA GSH.

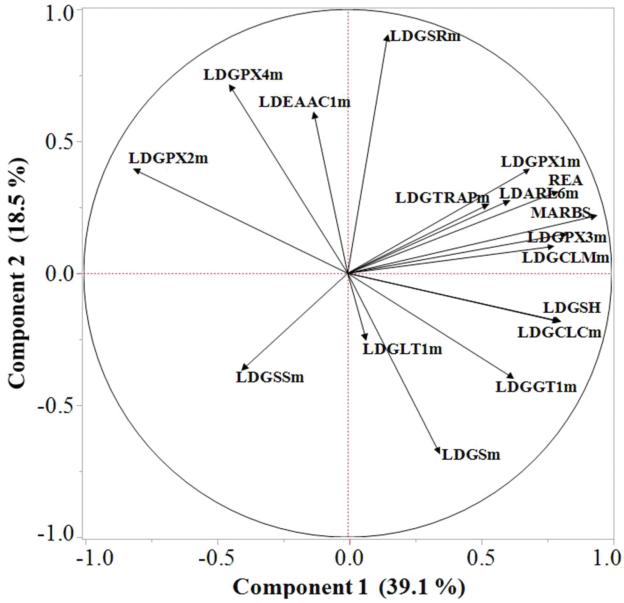

Figure 5. Loading plot from principal component analysis of steer (Growing and Finished steers) LD tissue showing the correlation of the first two principal components (Components 1 and 2) among GSH content, REA, and marbling score (MARBS) and relative mRNA content associated with enzymes affecting GSH content. LD, longissimus dorsi; m, mRNA; ARL6, ARL6IP1; EAAC1, excitatory amino acid carrier 1; GCLC, γ-glutamate-cysteine ligase catalytic subunit; GCLM, γ-glutamate-cysteine ligase modifier subunit; GGT1, γ-glutamyltranspeptidase 1; GLT1, glutamate transporter 1; GPX, glutathione peroxidase; GS, glutamine synthetase; GSH, glutathione; GSS, glutathione synthetase; GSR, GSSG reductase; GTRAP, GTRAP3-18.

Several GSH-utilizing enzymes guard cells against oxidative injury by scavenging reactive oxygen species and nitrogen radicals. In the cytosol and mitochondria, superoxide dismutase catalyzes the dismutation of superoxide radical (O_2^-) into H_2O_2, which is subsequently reduced into water and oxygen by catalase in peroxisomes (Salvi et al., 2007). The antioxidant function of GSH is catalyzed by GSH-using GSH peroxidases (e.g., GPX1-4), which reduce lipid peroxides and hydrogen peroxide into their corresponding alcohols and water. The expression patterns of GPX1 (ubiquitous, considered the "emergency" GPX to counteract hydroperoxide-induced oxidative stress), GPX2 (functions similarly to GPX1), GPX3 (the "extracellular" GPX with GPX1-like and lipid hydroperoxidase activity), and GPX4 (broad specificity as the "phospholipid hydroperoxidase" GPX) are not fully characterized and can vary by species (Flohe, 2012). In the matrix space of mitochondria and the cytosol, GPX1 use of GSH is especially important in defending against oxidative stress (Fernandez-Checa et al., 1997; Lu, 2013). The resulting disulfide-oxidized form of GSH (GSSG) is reduced back into two molecules of GSH by GSSG reductase, thereby completing a redox cycle (Lu, 2013). GSH also is used by the glutathione-S-transferases (e.g., GSTM1) to conjugate GSH to xenobiotics for the purpose of detoxification (Schmidt and Dringen, 2012).

γ-Glutamyltranspeptidase (GGT) is the only enzyme known to be cable of hydrolyzing the γ-carboxyl-amine bond of GSH, thereby initiating the breakdown of extracellular GSH to supply the rate-limiting amino acid (Cys) for intracellular GSH synthesis (Lu, 2013). γ-Glutamyltranspeptidase activity is highest in tubule epithelia (Deneke and Fanburg, 1989) and lower in brain, liver, and skeletal muscle (Leeuwenburgh et al., 1994; Brown-Borg and Rakoczy, 2005).

Although it would have been more informative to determine the ratio of oxidized (GSSG) to reduced GSH (GSH) as an indicator of oxidative stress (Asensi et al., 1999), a decrease in tissue GSH content typically is interpreted to mean that the tissue is experiencing increased oxidative stress due to an increased metabolism (Jankovic et al., 2014). The decreased GSH content of skeletal muscle and adipose tissues in obese mice and humans has been documented (Anderson et al., 2009; Jankovic et al., 2014). In cattle, however, it is not known whether the GSH content changes in skeletal muscle and adipose tissues as animals fatten and, if so, how this process occurs. Therefore, the first goal was to test the hypothesis that the GSH content would be reduced in the 12th to 13th rib LD and SA tissues of Finished vs. Growing beef steers due to their relatively greater adipose accretion. Also unknown is whether the capacity for liver GSH production and secretion changes, to support changes in hepatic and peripheral tissue metabolism. The second goal was to gain insight into how tissue-specific GSH content is achieved by comparing the relative expression patterns of selective GSH-associated transporters and metabolizing proteins in LD, SA, and liver tissues. The growth and carcass characteristics of the steers used in this study have been reported (Huang et al., 2018) and are representative of commercial growing and finished phenotypes.

Liver GSH Content Did Not Differ Between Steer Phenotypes, Consistent with Decreased GSH Synthesis and Export, and Increased Xenobiotic Detoxification Potential

Although most cell types can synthesize GSH, liver-synthesized GSH is the major source of GSH for most peripheral tissues (Deneke and Fanburg, 1989; Lu, 2013). Within the liver, GSH is synthesized in the pericentral hepatocytes, the same cells where system X_{AG}^- transporters and GS are localized

(Häussinger and Gerok, 1983; Boon et al., 1999; Braeuning et al., 2006). Thus, γ-glutamylcysteine ligase and GS may directly compete for Glu. After synthesis, GSH is exported into the blood and bile by ABCC1, SLCO1B3, or SLCO2B1. Plasma GSH can also be utilized by other organs such as lung and intestinal epithelium with high levels of GGT activity (Deneke and Fanburg, 1989). Because the liver is a net exporter of GSH, depletion of liver GSH under increased oxidative stress or xenobiotic metabolism may result in a depleted supply of GSH for use by other tissues. Accordingly, hepatic GSH production and secretion play a critical role in the whole animal GSH homeostasis (Lauterburg et al., 1984; Deneke and Fanburg, 1989).

The liver tissue GSH content was about 1.07 mg/g wet tissue and did not differ between Finished and Growing steers (Table 5; Huang et al., 2018). At this level, hepatic GSH content was about 3- and 2-fold more than that of LD (Table 1), and 7- and 13-fold greater than that of SA (Table 3), tissues of Growing and Finished steers, respectively. However, it should be noted that these comparisons do not account for differences in dry matter and protein content among these tissues. The capacity for system X^-_{AG} activity-dependent uptake of Glu and Cys from blood by the liver was decreased in Finished steers (Huang et al., 2018). Concomitantly, Finished steers expressed less GSH-synthesizing potential due to less GCLC and GSS mRNA, whereas GCLM and GSR expression did not differ (Table 5). Collectively, these results suggest a decreased GSH synthesis capacity in the liver tissue of Finished steers. In apparent accordance with the reduced GSH synthesis capacity, the decreased content of mRNA for GSH exporters ABCC1 (40%), SLCO1B3 (32%), and SLCO2B1 (61%) suggests a decreased GSH efflux capacity in the liver of Finished vs. Growing steers.

For GSH-metabolizing proteins, the decreased GPX1 expression in the liver of Finished steers (Table 5) indicates a decreased demand for GSH, and a decreased capacity to reduce hydrogen peroxide as steers fattened. In contrast, the 100% increase in GSTM1 mRNA content in Finished steers suggests that they had a greater demand for GSH, and a greater capacity for detoxification of xenobiotics (Schmidt and Dringen, 2012).

Steady-state cellular GSH content results from the amount produced versus the amount utilized and exported out of the cell. Although it remains to be experimentally determined, if the shifts in the relative abundance of mRNA and protein of assessed transporters and enzymes corresponds to actual changes in metabolic capacities, then the tissue-specific differential expression patterns of GSH-related enzymes and transporters appear consistent with the equal GSH content in the liver of Finished and Growing steers.

The Increased Content of GSH in LD of Finished Steers Is Consistent with an Increased Potential for GSH Synthesis

Because of its integral physiological role and economic importance in carcass evaluation, and its presumed relationship with intramuscular adipose content, the LD was studied as the model for skeletal muscle tissue. As reported previously, both the REA (53 vs. 77 cm^2) and marbling scores (296 vs. 668) were greater in Finished than Growing steers, respectively (Huang et al., 2018). The GSH content also was greater in the LD tissue of Finished steers (Table 1), in keeping with our hypothesis and indicative of a net antioxidant content, thus decreased oxidative stress (Aoyama et al., 2006; Findeisen et al., 2011; Aoyama and Nakaki, 2012). Moreover, PCA clearly indicated that REA and marbling score, as well as SA thickness, YG, and HCW, were more correlated with LD GSH content than GSH content of SA or liver tissues (Fig. 4).

Ostensibly, the greater LD GSH content resulted from an increased capacity for GSH synthesis, a decreased demand for GSH, or both. In this regard, an adequate supply of plasma Glu is necessary to support GSH and Gln metabolism by skeletal muscle (Hack et al., 1996; Ushmorov et al., 1999). In the mouse neuronal model, EAAC1 delivers substrates to support Gln (Glu) and GSH (Glu, Cys) synthesis (Aoyama et al., 2006), unless EAAC1 activity is inhibited by binding by endoplasmic reticulum–localized GTRAP3-18, thereby delaying the trafficking of EAAC1 to the plasma membrane (Lin et al., 2001; Ruggiero et al., 2008). In turn, GTRAP3-18 function is inhibited when bound by ARL6IP1, resulting in increased EAAC1 activity and GSH synthesis.

Although GTRAP3-18 regulation of EAAC1 is established for brain tissue, knowledge about the relationship between EAAC1, GTRAP3-18, and ARL6IP1 expression and GSH content and glutamine synthesis activity in peripheral tissues is limited. In cattle, hepatic GTRAP3-18 protein content is increased in aged vs. young cows, concomitant with decreased EAAC1 and GS (Miles et al., 2015). Importantly, the liver of Finished steers had decreased Glu transport and Gln synthesis capacities concomitant with increased GTRAP3-18 and

ARL6IP1 content, and no difference in GSH content (Huang et al., 2018). In contrast, the GSH content in the LD of Finished steers was greater, concomitant with no change in GTRAP3-18 and ARL6IP1 content and decreased EAAC1 and GS content (Table 1). Thus, different regulators may control EAAC1 and GS in LD vs. liver tissue. Moreover, that GSH content was greater in the LD of Finished steers, despite a reduced EAAC1 content, suggests that the increase in GSH content was not related to EAAC1-mediated Glu and Cys supply. Although not measured, the increased blood supply of Cys to support the increased GSH content may have resulted from an increased activity of system x_c^-, which exchanges one molecule of extracellular cystine (2 Cys) for one molecule of intracellular Glu (Griffith, 1999). Whether the observed reduced GS content suggests that there was less of a need for Glu to support GS-mediated Gln synthesis, or is a reflection of less Glu being available as a substrate of GS, remains to be determined.

Also consistent with the apparent reduced capacity for EAAC1-mediated uptake of Glu and Cys in the LD tissue of Finished steers, yet increased GSH content, was the increased mRNA content of γ-glutamyltranspeptidase (GGT1, 65%) to supply Glu and Cys for GSH, concomitant with an increased potential to synthesize GSH with increased GCLC (60%), and GCLM (28%) (Table 2). That is, the LD of Finished steers appeared to have a greater potential to synthesize GSH from blood-borne, liver-derived GSH than did Growing steers.

With regard to an altered potential to use GSH as an antioxidant, the LD tissue of Finished steers had more GPX1 (42%) and GPX3 (80%) mRNA content, indicating a greater capacity than Growing steers to metabolize hydrogen peroxide and fatty acid hydroperoxides (Thomas et al., 1990; Esworthy et al., 1991). Conversely, GPX2 mRNA content was decreased (50%), suggesting a reduced potential to metabolize organic hydroperoxides (Chu et al., 1993). Collectively, the measured differences in mRNA and protein contents of Glu and Cys acquiring and GSH-synthesizing and metabolizing enzymes, and increased GSH content, indicate that the LD tissue of Finished steers had an increased net antioxidant capacity, consistent with the measured increased GSH content. Moreover, PCA (Fig. 5) indicated that expression of genes responsible for initiating GSH synthesis (GCLC and GCLM) may be more responsible for GSH content in LD tissue, REA, and marbling score than other genes associated with GSH production (GSS and GSR).

The Decreased Content of GSH in SA Tissue Is Consistent with a Decreased Potential to Acquire Constituent AA and Increased GPX3 Expression

Because of its importance in carcass evaluation, known role as a net producer of Gln (Frayn et al., 1991), and presumed contribution to whole-body redox potential (Galinier et al., 2006; Chattopadhyay et al., 2015), SA was selected as the adipose tissue to study, despite reports that visceral adipose tissue has a greater GSH-mediated metabolism (Jankovic et al., 2014). In addition, the 12th to 13th rib SA tissue of steers expresses EAAC1 from weanling to finished production stages (Matthews et al., 2016). As reported previously (Huang et al., 2018), the 12th to 13th rib adipose thickness increased from 0.54 to 1.73 cm as steers developed from growing into finished phenotypes.

As hypothesized, the GSH content of SA tissue decreased 38% in Finished vs. Growing steers (Table 3). This decreased GSH content is consistent with the production of high concentrations of reactive species resulting from increased adipogenesis (Aoyama et al., 2006; Findeisen et al., 2011; Aoyama and Nakaki, 2012). Also, or alternatively, the potential for intracellular GSH synthesis may have been less in the SA tissue of Finished steers. For example, the increased content of GTRAP3-18 may have resulted in decreased EAAC1 activity, resulting in a decreased capacity to take up system X_{AG}^--mediated Glu and Cys from blood. This finding is consistent with previous studies showing that increased GTRAP3-18 inhibits cellular GSH content through inhibition of EAAC1 activity in human embryonic kidney 293 cells (Watabe et al., 2007) and that suppression of GTRAP3-18 increases neuronal GSH content in GTRAP3-18$^{-/-}$ mice (Aoyama and Nakaki, 2012). Assuming that the increased GTRAP3-18 content resulted in decreased EAAC1 transport activity, as it did in the livers of these Finished steers (Huang et al., 2018), this finding suggests that EAAC1 activity was decreased in SA of Finished steers. Moreover, that GGT1 mRNA content also was decreased 70% (Table 4), suggests a decreased capacity to recycle extracellular GSH to support intracellular GSH synthesis in Finished vs. Growing steers.

Based on these findings, the SA tissue of Finished steers may have had a reduced capacity for supplying GSH constituents from the blood. However, this apparent reduced capacity was not accompanied by a compensating change in reduced expression of metabolizing enzymes, except for a 50% reduction in GPX4 (Table 4). The decreased

GPX4 mRNA suggests a decreased ability to catalyze the reduction of phospholipid-, cholesterol-, and linoleic acid-hydroperoxides (Maiorino et al., 1990) when steers develop from growing to finishing stage, consistent with a decreased GSH content. This result is somewhat surprising given the reported relatively high pentose-phosphate pathway activity of bovine (Miller et al., 1991) and other species adipocytes (Galinier, et al., 2006), thus an enhanced capacity to support NADPH-dependent reduction of oxidized GSH to reduced GSH by GSSG reductase (for which expression did not change). Regardless of the mechanism, that the GSH content was lower in the SA tissue of Finished steers is consistent with an increased antioxidant stress (Jankovic et al., 2014), resulting from fatty acid synthesis-induced generation of radical oxygen species (Smith, 1995).

In conclusion, this research revealed tissue-specific responses in GSH content to fattening among the liver, LD, and SA tissues of beef steers as they developed from predominately lean to predominately lipid phenotypes. This research also revealed novel mechanistic knowledge about tissue-specific changes in the pattern of gene and protein expression of enzymes and transporters that influence GSH content. Three especially salient findings were that the GSH content was greater, not less, in the LD of Finished vs. Growing steers, was more correlated with REA and marbling scores than in liver or SA tissues, and among genes responsible for GSH synthesis, GCLC and GCLM appeared more correlated with GSH content in LD tissue, REA, and marbling score. Second, the potential to support GSH production in SA tissue appeared to be lower in Finished steers. Third, the EAAC1 regulatory proteins GTRAP3-18 and ARL6IP1 are expressed by LD and SA tissues, and their relationship to GSH, EAAC1, and GS content differs and changes as Growing steers develop into Finished steer phenotypes.

SUPPLEMENTARY DATA

Supplementary data are available at *Journal of Animal Science* online.

Conflict of interest statement. None declared.

LITERATURE CITED

Anderson, E. J., M. E. Lustig, K. E. Boyle, T. L. Woodlief, D. A. Kane, C. T. Lin, J. W. Price, III, L. Kang, P. S. Rabinovitch, H. H. Szeto, et al. 2009. Mitochondrial H_2O_2 emission and cellular redox state link excess fat intake to insulin resistance in both rodents and humans. J. Clin. Invest. 119:573–581. doi:10.1172/JCI37048

Asensi, M., J. Sastre, F. V. Pallardo, A. Lloret, M. Lehner, J. Garcia-de-la Asuncion, and J. Viña. 1999. Ratio of reduced to oxidized glutathione as indicator of oxidative stress status and DNA damage. Methods Enzymol. 299:267–276.

Aoyama, K., and T. Nakaki. 2012. Inhibition of GTRAP3-18 may increase neuroprotective glutathione (GSH) synthesis. Int. J. Mol. Sci. 13:12017–12035. doi:10.3390/ijms130912017

Aoyama, K., S. W. Suh, A. M. Hamby, J. Liu, W. Y. Chan, Y. Chen, and R. A. Swanson. 2006. Neuronal glutathione deficiency and age-dependent neurodegeneration in the EAAC1 deficient mouse. Nat. Neurosci. 9:119–126. doi:10.1038/nn1609

Aoyama, K., M. Watabe, and T. Nakaki. 2008. Regulation of neuronal glutathione synthesis. J. Pharmacol. Sci. 108:227–238.

Boon, L., W. J. Geerts, A. Jonker, W. H. Lamers, and C. J. Van Noorden. 1999. High protein diet induces pericentral glutamate dehydrogenase and ornithine aminotransferase to provide sufficient glutamate for pericentral detoxification of ammonia in rat liver lobules. Histochem. Cell Biol. 111:445–452.

Braeuning, A., C. Ittrich, C. Köhle, S. Hailfinger, M. Bonin, A. Buchmann, and M. Schwarz. 2006. Differential gene expression in periportal and perivenous mouse hepatocytes. Febs J. 273:5051–5061. doi:10.1111/j.1742-4658.2006.05503.x

Brown, K. R., G. A. Anderson, K. Son, G. Rentfrow, L. P. Bush, J. L. Klotz, J. R. Strickland, J. A. Boling, and J. C. Matthews. 2009. Growing steers grazing high versus low endophyte (*Neotyphodium coenophialum*)-infected tall fescue have reduced serum enzymes, increased hepatic glucogenic enzymes, and reduced liver and carcass mass. J. Anim. Sci. 87:748–760. doi:10.2527/jas.2008-1108

Brown-Borg, H. M., and S. G. Rakoczy. 2005. Glutathione metabolism in long-living Ames dwarf mice. Exp. Gerontol. 40:115–120. doi:10.1016/j.exger.2004.11.004

Chattopadhyay, M., V. K. Khemka, G. Chatterjee, A. Ganguly, S. Mukhopadhyay, and S. Chakrabarti. 2015. Enhanced ROS production and oxidative damage in subcutaneous white adipose tissue mitochondria in obese and type 2 diabetes subjects. Mol. Cell. Biochem. 399:95–103. doi:10.1007/s11010-014-2236-7

Chen, Y., H. G. Shertzer, S. N. Schneider, D. W. Nebert, and T. P. Dalton. 2005. Glutamate cysteine ligase catalysis: dependence on ATP and modifier subunit for regulation of tissue glutathione levels. J. Biol. Chem. 280:33766–33774. doi:10.1074/jbc.M504604200

Chu, F. F., J. H. Doroshow, and R. S. Esworthy. 1993. Expression, characterization, and tissue distribution of a new cellular selenium-dependent glutathione peroxidase, GSHPx-GI. J. Biol. Chem. 268:2571–2576.

Deneke, S. M., and B. L. Fanburg. 1989. Regulation of cellular glutathione. Am. J. Physiol. 257:L163–L173. doi:10.1152/ajplung.1989.257.4.L163

Elsasser, T. H., T. J. Caperna, C. J. Li, S. Kahl, and J. L. Sartin. 2008. Critical control points in the impact of the proinflammatory immune response on growth and metabolism. J. Anim. Sci. 86 (14 Suppl):E105–E125. doi:10.2527/jas.2007-0634

Esworthy, R. S., F. F. Chu, R. J. Paxton, S. Akman, and J. H. Doroshow. 1991. Characterization and partial amino acid sequence of human plasma glutathione peroxidase. Arch. Biochem. Biophys. 286:330–336.

Fan, M. Z., J. C. Matthews, N. M. Etienne, B. Stoll, D. Lackeyram, and D. G. Burrin. 2004. Expression of apical membrane L-glutamate transporters in neonatal porcine epithelial cells along the small intestinal crypt-villus axis. Am. J. Physiol. Gastrointest. Liver Physiol. 287:G385–G398. doi:10.1152/ajpgi.00232.2003

Fernandez-Checa, J. C., N. Kaplowitz, C. García-Ruiz, A. Colell, M. Miranda, M. Marí, E. Ardite, and A. Morales. 1997. GSH transport in mitochondria: defense against TNF-induced oxidative stress and alcohol-induced defect. Am. J. Physiol. 273:G7–G17. doi:10.1152/ajpgi.1997.273.1.G7

Findeisen, H. M., K. J. Pearson, F. Gizard, Y. Zhao, H. Qing, K. L. Jones, D. Cohn, E. B. Heywood, R. de Cabo, and D. Bruemmer. 2011. Oxidative stress accumulates in adipose tissue during aging and inhibits adipogenesis. Plos One 6:e18532. doi:10.1371/journal.pone.0018532

Flaring, U. B., O. E. Rooyackers, J. Wernerman, and F. Hammarqvist. 2003. Glutamine attenuates post-traumatic glutathione depletion in human muscle. Clin. Sci. (Lond). 104:275–282. doi:10.1042/CS20020198

Flohe L. 2012. Glutathione peroxidases. In: J. Liu, G. Luo, and Y. Mu, editors, Selenoproteins and mimics. Zhejiang University Press, Hangzhou and Springer, New York, p. 1–25.

Forman, H. J., H. Zhang, and A. Rinna. 2009. Glutathione: overview of its protective roles, measurement, and biosynthesis. Mol. Aspects Med. 30:1–12. doi:10.1016/j.mam.2008.08.006

Franklin, C. C., D. S. Backos, I. Mohar, C. C. White, H. J. Forman, and T. J. Kavanagh. 2009. Structure, function, and post-translational regulation of the catalytic and modifier subunits of glutamate cysteine ligase. Mol. Aspects Med. 30:86–98. doi:10.1016/j.mam.2008.08.009

Frayn, K. N., K. Khan, S. W. Coppack, and M. Elia. 1991. Amino acid metabolism in human subcutaneous adipose tissue in vivo. Clin. Sci. (Lond). 80:471–474.

Furukawa, S., T. Fujita, M. Shimabukuro, M. Iwaki, Y. Yamada, Y. Nakajima, O. Nakayama, M. Makishima, M. Matsuda, and I. Shimomura. 2017. Increased oxidative stress in obesity and its impact on metabolic syndrome. J. Clin. Invest. 114:1752–1761. doi:10.1172/JCI21625

Galinier, A., A. Carrière, Y. Fernandez, C. Carpéné, M. André, S. Caspar-Bauguil, J. P. Thouvenot, B. Périquet, L. Pénicaud, and L. Casteilla. 2006. Adipose tissue proadipogenic redox changes in obesity. J. Biol. Chem. 281:12682–12687. doi:10.1074/jbc.M506949200

Griffith, O. W. 1999. Biologic and pharmacologic regulation of mammalian glutathione synthesis. Free Radic. Biol. Med. 27:922–935.

Hack, V., O. Stütz, R. Kinscherf, M. Schykowski, M. Kellerer, E. Holm, and W. Dröge. 1996. Elevated venous glutamate levels in (pre)catabolic conditions result at least partly from a decreased glutamate transport activity. J. Mol. Med. (Berl). 74:337–343.

Häussinger, D., and W. Gerok. 1983. Hepatocyte heterogeneity in glutamate uptake by isolated perfused rat liver. Eur. J. Biochem. 136:421–425.

Howell, J. A., A. D. Matthews, K. C. Swanson, D. L. Harmon, and J. C. Matthews. 2001. Molecular identification of high-affinity glutamate transporters in sheep and cattle forestomach, intestine, liver, kidney, and pancreas. J. Anim. Sci. 79:1329–1336.

Howell, J. A., A. D. Matthews, T. C. Welbourne, and J. C. Matthews. 2003. Content of ileal EAAC1 and hepatic GLT-1 high-affinity glutamate transporters is increased in growing vs. nongrowing lambs, paralleling increased tissue D- and L-glutamate, plasma glutamine, and alanine concentrations. J. Anim. Sci. 81:1030–1039. doi:10.2527/2003.8141030x

Huang, C. S., M. E. Anderson, and A. Meister. 1993a. Amino acid sequence and function of the light subunit of rat kidney gamma-glutamylcysteine synthetase. J. Biol. Chem. 268:20578–20583.

Huang, C. S., L. S. Chang, M. E. Anderson, and A. Meister. 1993b. Catalytic and regulatory properties of the heavy subunit of rat kidney gamma-glutamylcysteine synthetase. J. Biol. Chem. 268:19675–19680.

Huang, J., Y. Jia, Q. Li, W. R. Burris, P. J. Bridges, and J. C. Matthews. 2018. Hepatic glutamate transport and glutamine synthesis capacities are decreased in finished vs. growing beef steers, concomitant with increased GTRAP3-18 content. Amino Acids 50:513–525. doi:10.1007/s00726-018-2540-8

Jankovic, A., A. Korac, B. Srdic-Galic, B. Buzadzic, V. Otasevic, A. Stancic, M. Vucetic, M. Markelic, K. Velickovic, I. Golic, et al. 2014. Differences in the redox status of human visceral and subcutaneous adipose tissues–relationships to obesity and metabolic risk. Metabolism. 63:661–671. doi:10.1016/j.metabol.2014.01.009

Kilberg, M. S. 1989. Measurement of amino acid transport by hepatocytes in suspension or monolayer culture. Methods Enzymol. 173:564–575.

Lauterburg, B. H., J. D. Adams, and J. R. Mitchell. 1984. Hepatic glutathione homeostasis in the rat: efflux accounts for glutathione turnover. Hepatology 4:586–590.

Leeuwenburgh, C., R. Fiebig, R. Chandwaney, and L. L. Ji. 1994. Aging and exercise training in skeletal muscle: responses of glutathione and antioxidant enzyme systems. Am. J. Physiol. 267:R439–R445. doi:10.1152/ajpregu.1994.267.2.R439

Lin, C. I., I. Orlov, A. M. Ruggiero, M. Dykes-Hoberg, A. Lee, M. Jackson, and J. D. Rothstein. 2001. Modulation of the neuronal glutamate transporter EAAC1 by the interacting protein GTRAP3-18. Nature 410:84–88. doi:10.1038/35065084

Livak, K. J., and T. D. Schmittgen. 2001. Analysis of relative gene expression data using real-time quantitative PCR and the 2(-delta delta C(T)) method. Methods 25:402–408. doi:10.1006/meth.2001.1262

Lu, S. C. 2013. Glutathione synthesis. Biochim. Biophys. Acta 1830:3143–3153. doi:10.1016/j.bbagen.2012.09.008

Maiorino, M., C. Gregolin, and F. Ursini. 1990. Phospholipid hydroperoxide glutathione peroxidase. Methods Enzymol. 186:448–457.

Matthews, J. C., J. Huang, and G. Rentfrow. 2016. High-affinity glutamate transporter and glutamine synthetase content in longissimus dorsi and adipose tissues of growing angus steers differs among suckling, weanling, backgrounding, and finishing production stages. J. Anim. Sci. 94:1267–1275. doi:10.2527/jas.2015-9901

Miles, E. D., B. W. McBride, Y. Jia, S. F. Liao, J. A. Boling, P. J. Bridges, and J. C. Matthews. 2015. Glutamine synthetase and alanine transaminase expression are decreased in livers of aged vs. young beef cows and GS can be upregulated by 17β-estradiol implants. J. Anim. Sci. 93:4500–4509. doi:10.2527/jas.2015-9294

Miller, M. F., H. R. Cross, D. K. Lunt, and S. B. Smith. 1991. Lipogenesis in acute and 48-hour cultures of bovine intramuscular and subcutaneous adipose tissue explants. J. Anim. Sci. 69:162–170.

Moisá, S. J., D. W. Shike, D. E. Graugnard, S. L. Rodriguez-Zas, R. E. Everts, H. A. Lewin, D. B. Faulkner, L. L. Berger, and J. J. Loor. 2013. Bioinformatics analysis of transcriptome dynamics during growth in angus cattle longissimus muscle. Bioinform. Biol. Insights 7:253–270. doi:10.4137/BBI.S12328

NRC. 1996. Energy. Nutrient Requirements of Beef Cattle. 7th rev. ed. National Academy Press, Washigton, DC, p. 3-15.

Noeman, S. A., H. E. Hamooda, and A. A. Baalash. 2011. Biochemical study of oxidative stress markers in the liver, kidney and heart of high fat diet induced obesity in rats. Diabetol. Metab. Syndr. 3:17. doi:10.1186/1758-5996-3-17

Richman, P. G., and A. Meister. 1975. Regulation of gamma-glutamyl-cysteine synthetase by nonallosteric feedback inhibition by glutathione. J. Biol. Chem. 250:1422–1426.

Ruggiero, A. M., Y. Liu, S. Vidensky, S. Maier, E. Jung, H. Farhan, M. B. Robinson, H. H. Sitte, and J. D. Rothstein. 2008. The endoplasmic reticulum exit of glutamate transporter is regulated by the inducible mammalian Yip6b/GTRAP3-18 protein. J. Biol. Chem. 283:6175–6183. doi:10.1074/jbc.M701008200

Salvi, M., V. Battaglia, A. M. Brunati, N. La Rocca, E. Tibaldi, P. Pietrangeli, L. Marcocci, B. Mondovì, C. A. Rossi, and A. Toninello. 2007. Catalase takes part in rat liver mitochondria oxidative stress defense. J. Biol. Chem. 282:24407–24415. doi:10.1074/jbc.M701589200

Sato, H., M. Tamba, T. Ishii, and S. Bannai. 1999. Cloning and expression of a plasma membrane cystine/glutamate exchange transporter composed of two distinct proteins. J. Biol. Chem. 274:11455–11458.

Schmidt, M. M., and R. Dringen. 2012 Glutathione (GSH) Synthesis and Metabolism. In: I. Y. Choi and R. Gruetter, editors, Neural metabolism in vivo. Advances in neurobiology, vol 4. Springer, Boston, MA. p. 1029-1050.

Sies, H., C. Berndt, and D. P. Jones. 2017. Oxidative stress. Annu. Rev. Biochem. 86:715–748. doi:10.1146/annurev-biochem-061516-045037

Smith, S. B. 1995. Substrate utilization in ruminant adipose tissues. In: S. B. Smith and D. R. Smith, editors, The biology of fat in meat animals: current advances. Am. Soc. Anim. Sci., Champaign, IL. p. 166–188.

Swanson, K. C., J. C. Matthews, A. D. Matthews, J. A. Howell, C. J. Richards, and D. L. Harmon. 2000. Dietary carbohydrate source and energy intake influence the expression of pancreatic alpha-amylase in lambs. J. Nutr. 130:2157–2165. doi:10.1093/jn/130.9.2157

Thomas, J. P., M. Maiorino, F. Ursini, and A. W. Girotti. 1990. Protective action of phospholipid hydroperoxide glutathione peroxidase against membrane-damaging lipid peroxidation. In situ reduction of phospholipid and cholesterol hydroperoxides. J. Biol. Chem. 265:454–461.

USDA. 1997. Unites states standards for beef carcasses. Livet. Seed Program, Agric. Market. Serv., Des Moines, IA.

Ushmorov, A., V. Hack, and W. Dröge. 1999. Differential reconstitution of mitochondrial respiratory chain activity and plasma redox state by cysteine and ornithine in a model of cancer cachexia. Cancer Res. 59:3527–3534.

Vincent, H. K., K. E. Innes, and K. R. Vincent. 2007. Oxidative stress and potential interventions to reduce oxidative stress in overweight and obesity. Diabetes. Obes. Metab. 9:813–839. doi:10.1111/j.1463-1326.2007.00692.x

Watabe, M., K. Aoyama, and T. Nakaki. 2007. Regulation of glutathione synthesis via interaction between glutamate transport-associated protein 3-18 (GTRAP3-18) and excitatory amino acid carrier-1 (EAAC1) at plasma membrane. Mol. Pharmacol. 72:1103–1110. doi:10.1124/mol.107.039461

Watabe, M., K. Aoyama, and T. Nakaki. 2008. A dominant role of GTRAP3-18 in neuronal glutathione synthesis. J. Neurosci. 28:9404–9413. doi:10.1523/JNEUROSCI.3351-08.2008

Xue, Y., S. F. Liao, J. R. Strickland, J. A. Boling, and J. C. Matthews. 2011. Bovine neuronal vesicular glutamate transporter activity is inhibited by ergovaline and other ergopeptines. J. Dairy Sci. 94:3331–3341. doi:10.3168/jds.2010-3612

Yang, Y., M. Z. Dieter, Y. Chen, H. G. Shertzer, D. W. Nebert, and T. P. Dalton. 2002. Initial characterization of the glutamate-cysteine ligase modifier subunit gclm(-/-) knockout mouse. Novel model system for a severely compromised oxidative stress response. J. Biol. Chem. 277:49446–49452. doi:10.1074/jbc.M209372200